Smart Antenna Arrays for Correlated and Imperfectly-Estimated Rayleigh Fading Channels

Constantin Siriteanu and Steven D. Blostein

Department of Electrical and Computer Engineering
Queen's University, Kingston, Ontario, K7L3N6, Canada
e-mails: costi@ee.queensu.ca, sdb@ee.queensu.ca

Abstract— **Eigenbeamforming, herein referred to as *maximal-ratio eigen-combining* (MREC), was recently proposed as an alternative to maximum average signal-to-noise ratio beamforming (Max-ASNR BF) and maximal-ratio combining (MRC) in antenna array systems. An analysis of MREC is undertaken and an average error probability (AEP) expression is obtained for BPSK modulation and Rayleigh fading when the channel gains may be imperfectly-known and partially correlated. The analysis is further specialized to pilot-symbol-aided channel estimation, to allow an analytical performance assessment of smart antenna arrays (SAAs) employing MREC in realistic scenarios with angle-of-arrival (AOA) dispersion. Numerical results show that MREC may significantly outperform Max-ASNR BF and MRC in imperfect conditions.**

I. Introduction

Antenna arrays can increase range and user capacity in mobile wireless communication systems by combating multipath fading, interference and noise. To this end, signal processing performed by smart antenna arrays (SAAs) should account for the correlations between the channel gains, which are determined by the inter-element distance and by the angle-of-arrival (AOA) distribution type and parameters [1]. Conventional signal processing methods applied at receiving antenna arrays include: (1) maximum **average signal-to-noise ratio** beamforming (**Max-ASNR BF**) [2], for highly-correlated signals; (2) maximum **instantaneous signal-to-noise ratio** or maximal-ratio combining (**MRC**) [3], for highly-decorrelated signals. The symbol-detection performance degrades for both Max-ASNR BF [4] and MRC [3] for partially-correlated channel gains. Eigenbeamforming [5], which we refer to as *maximal-ratio eigen-combining* (MREC) [6] [7], incorporates the principles of Max-ASNR BF and MRC, by using long- and short-term (relative to the fading rate) channel features, to provide both antenna and diversity gains.

In principle, MREC employs the Karhunen-Loève Transform (KLT) [8] to obtain a minimum-loss lower-dimensional approximation of the received signal vector, followed by MRC, to take advantage of the effective diversity order with minimum complexity. Previously, MREC for imperfect channel knowledge was investigated only for *approximate* "maximal-ratio combining" where estimates of the transformed channel gains are used as actual weights [4] [6] [7] [9]. Approximate MREC was found to benefit SAAs in scenarios with significantly-correlated channel gains: (1) it yields diversity gain and reduces the average error probability (AEP) compared to the less complex Max-ASNR BF [4] [6] [7], (2) it reduces the short-term processing volume and improves the estimation precision compared to MRC [5] [6] [7] [9], and (3) it can be adapted to the actual environment scattering characteristics, unlike Max-ASNR BF and MRC [7].

In this work we investigate MREC for imperfect channel knowledge when the second step in MREC consists of *exact* maximal-ratio combining, as described in [10]. Exact MREC is optimal, easier to analyze than approximate MREC [6] and can provide a natural criterion for adaptive MREC order selection [7]. In Section II, partial correlation between channel gains, induced by moderate AOA dispersion at antenna arrays, is shown to lead to MREC by integrating concepts from Max-ASNR BF and MRC. Section III contains an AEP-analysis of exact MREC for BPSK transmission and imperfectly-estimated Rayleigh fading channel, which is further specialized to the case of estimation based on pilot-symbol-aided modulation [11] (PSAM). Numerical results obtained from analysis and simulations show in Section IV that MREC may significantly outperform Max-ASNR BF and MRC.

II. Signal processing for SAAs

Consider a base station with an N-element antenna array receiving a BPSK-modulated signal transmitted by a single mobile station, after propagation through a frequency-flat Rayleigh fading channel. After demodulation, matched-filtering and sampling, the complex-valued received signal vector can be written as:

$$\mathbf{y} = \sqrt{E_b}\, b\, \mathbf{h} + \mathbf{n} \tag{1}$$

where E_b is the energy transmitted per symbol and $b \in \{\pm 1\}$ is an equiprobable binary random variable. Assume that the (column) *channel vector* $\mathbf{h} = [h_1\, h_2\, \ldots\, h_N]^{\mathcal{T}}$ is the superposition of P temporally-unresolvable multipaths [1] [4]

[5] as in

$$\mathbf{h} = \frac{1}{\sqrt{P}} \sum_{p=1}^{P} g_p \, \mathbf{a}(\theta_c + \theta_p), \tag{2}$$

where g_p, θ_p and $\mathbf{a}(\theta_c + \theta_p)$ are, respectively, the random zero-mean complex channel gain, the random deviation from the mean AOA θ_c, and the array propagation vector [2] for the pth multipath. For large P, the components of the channel vector, h_i, $i = \overline{1, N} \triangleq 1, 2, \ldots, N$, denoted as channel gains and also as *branches* herein, are zero-mean Gaussian random variables [1]. In this section we assume the channel vector to be perfectly-known, unless specified otherwise. The *noise vector* $\mathbf{n}$ is assumed zero-mean, spatially-white complex Gaussian, $\mathbf{n} \sim \mathcal{N}(\mathbf{0}, N_0 \mathbf{I}_N)$. Furthermore, we assume that the transmitted symbols, channel gains and noise are statistically independent.

Since the channel vector correlation matrix $\mathbf{R_h} \triangleq E\{\mathbf{h}\,\mathbf{h}^{\mathcal{H}}\}$ obtained by averaging over fading is Hermitian, it has real and non-negative eigenvalues, $\lambda_1 \geq \lambda_2 \geq \ldots \geq \lambda_N \geq 0$, and a complete set of orthonormal eigenvectors, $\mathbf{e}_l$, $l = \overline{1, N}$. If we define $\mathbf{\Lambda} \triangleq \text{diag}\{\lambda_1, \lambda_2, \ldots, \lambda_N\}$ and the unitary matrix $\mathbf{E} \triangleq [\mathbf{e}_1\, \mathbf{e}_2 \ldots \mathbf{e}_N]$ then

$$\mathbf{R_h} = \mathbf{E}\mathbf{\Lambda}\mathbf{E}^{\mathcal{H}} = \sum_{l=1}^{N} \lambda_l \, \mathbf{e}_l \, \mathbf{e}_l^{\mathcal{H}}. \tag{3}$$

Throughout this work, we assume perfect knowledge of the eigen-structure of $\mathbf{R_h}$ since it can be accurately estimated in practice [5].

$\mathbf{R_h}$ and its eigen-structure reflect geometrical features of the antenna array as well as scattering [1]. For illustration purposes we will consider the following example setting: a 5-element uniform linear array (ULA) with half-wavelength spacing between adjacent elements; unitary channel gain variance, $E\{|h_l|^2\} = 1$, $l = \overline{1, N}$; uniformly-distributed AOA, $\theta = \theta_c + \theta_p$ (measured with respect to broadside), i.e. [1]

$$p(\theta) = \begin{cases} \frac{1}{2\Delta} & , \quad \text{if} \quad \theta \in [\theta_c - \Delta, \theta_c + \Delta] \\ 0 & , \quad \text{otherwise,} \end{cases} \tag{4}$$

where Δ is the maximum AOA dispersion; $\theta_c = 0$. Then, $\mathbf{R_h}$ can be computed using [1, Eqns. (A-19) and (A-20)]. For this setting, Fig. 1 depicts the dependence between Δ, the correlation between two adjacent channel vector components ρ, and the eigenvalues of $\mathbf{R_h}$, λ_l, $l = \overline{1, N}$.

The following hold in general and are reflected in Fig. 1.

***Fact** 1:* the elements of $\mathbf{h}$ are coherent (fully correlated) with $\mathbf{h} = \tilde{h}_1 \cdot \mathbf{e}_1$ (clearly, $\tilde{h}_1 = \mathbf{e}_1^{\mathcal{H}} \mathbf{h}$) if and only if (iff) [1] $\lambda_1 = \text{tr}(\mathbf{R_h})$ and $\lambda_2 = \lambda_3 = \ldots = \lambda_N = 0$.

***Fact** 2:* the elements of $\mathbf{h}$ are uncorrelated, i.e., $(\mathbf{R_h})_{l_1, l_2} \triangleq E\{h_{l_1} \, h_{l_2}^*\} = 0$, $\forall l_1, l_2 = \overline{1, N}, l_1 \neq l_2$, with equal variances $(\mathbf{R_h})_{l,l} \triangleq E\{|h_l|^2\} = \lambda$, $l = \overline{1, N}$, iff the eigenvalues of $\mathbf{R_h}$ are all equal, i.e., $\lambda_l = \lambda$, $l = \overline{1, N}$.

[1] $\text{tr}(\mathbf{R_h}) \triangleq \sum_{l=1}^{N} (\mathbf{R_h})_{l,l} = \sum_{l=1}^{N} \lambda_l$ is a measure of the total intended-signal energy received at the antenna array.

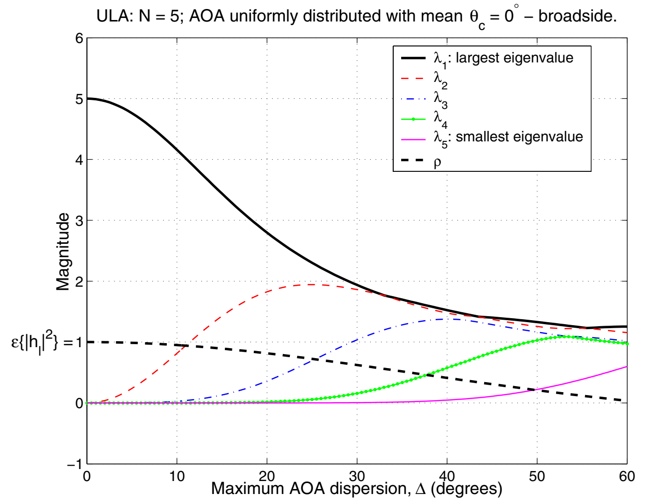

Fig. 1. Eigenvalues of $\mathbf{R_h}$ and fading correlation at two adjacent antenna elements vs. the maximum AOA dispersion.

For $\Delta = 0$, Fig. 1 suggests that $\mathbf{R_h}$ is rank-one. This can be proven analytically using first the channel model in (2) to show that the branches are coherent, and then Fact 1. The maximum-likelihood (ML) symbol detector in this case is given by

$$\hat{b}_{BF} = \text{sign}\left[\Re(\mathbf{w}_{BF}^{\mathcal{H}} \, \mathbf{y})\right], \; \mathbf{w}_{BF} = \mathbf{h} = \tilde{h}_1 \, \mathbf{e}_1, \; \tilde{h}_1 = \mathbf{e}_1^{\mathcal{H}} \, \mathbf{h} \tag{5}$$

where $\Re(\cdot)$ stands for the real part of a complex number. Since $\mathbf{w}_{BF}$ is proportional to the dominant eigenvector $\mathbf{e}_1$ of $\mathbf{R_h}$, it maximizes $\frac{\mathbf{w}^{\mathcal{H}} \mathbf{R_h} \mathbf{w}}{\mathbf{w}^{\mathcal{H}} \mathbf{w}}$, i.e., it yields maximum average SNR beamforming [2] (Max-ASNR BF). Max-ASNR BF has low complexity and also enhances the estimation precision for $\tilde{h}_1$ as a result of array gain [5].

Note that $\mathbf{w}_{BF} = \tilde{h}_1 \, \mathbf{e}_1$ always yields maximum average output SNR, even for nonzero AOA dispersion, i.e., when $\mathbf{h}$ is actually a linear combination of several eigenvectors of $\mathbf{R_h}$ — see Fig. 1. However, the Max-ASNR BF detector from (5) is then no longer ML, i.e., $\mathbf{w}_{BF} = \tilde{h}_1 \, \mathbf{e}_1 \neq \mathbf{h}$, and its performance is expected to degrade with increasing AOA dispersion [4].

Obviously, $\mathbf{w}_{ML} = \mathbf{h}$ is the ML combiner regardless of the AOA dispersion, i.e., branch correlation. It also maximizes the instantaneous output SNR [3] yielding MRC. Notice that, unlike Max-ASNR BF, MRC yields diversity gain, but requires knowledge of all elements of $\mathbf{h}$, which for an antenna with many elements means considerable processing for short-term channel estimation. Furthermore, not enough training symbols may lead to poor estimation accuracy which may significantly degrade MRC detection performance [5] [6] [7] [9]. Finally, MRC is known to offer minimum AEP only when the channel gains are uncorrelated [3] (situation described by Fact 2).

Fig. 1 shows that when the correlation between adjacent components of $\mathbf{h}$ is high ($\rho > 0.8$ [1]) only a few eigenvalues are significant, i.e., most of the intended-signal energy is confined to a subspace of fairly-low dimension. This observation lead to the maximal-ratio eigen-combining

(MREC) [5] approach in which a combiner is formed only with dominant eigenvectors of $\mathbf{R_h}$ in order to reduce the short-term processing complexity compared with MRC and to exploit the available diversity gain, unlike Max-ASNR BF.

The first step in MREC is to apply the KLT [8] matrix $\mathbf{E}_L^{\mathcal{H}} \triangleq [\mathbf{e}_1 \quad \mathbf{e}_2 \quad \ldots \quad \mathbf{e}_L]^{\mathcal{H}}$, for an appropriately-chosen $L = \overline{1, N}$ [7], to both sides of (1) to obtain

$$\tilde{\mathbf{y}}_L = \sqrt{E_b}\, b\, \tilde{\mathbf{h}}_L + \tilde{\mathbf{n}}_L, \tag{6}$$

where $\tilde{\mathbf{y}}_L \triangleq \mathbf{E}_L^{\mathcal{H}}\mathbf{y}, \tilde{\mathbf{h}}_L \triangleq \mathbf{E}_L^{\mathcal{H}}\mathbf{h}, \tilde{\mathbf{n}}_L \triangleq \mathbf{E}_L^{\mathcal{H}}\mathbf{n}$. The KLT is the optimum least-squares decorrelating transform [8], i.e., among all the possible transforms, it concentrates the largest amount of energy from the original channel vector $\mathbf{h}$ into $\tilde{\mathbf{h}}_L = \left[\tilde{h}_1 \ldots \tilde{h}_L\right]^{\mathcal{T}}$, with $\tilde{h}_l = \mathbf{e}_l^{\mathcal{H}}\mathbf{h}$, $l = \overline{1, L}$. The components of $\tilde{\mathbf{h}}_L$, further denoted as *eigenbranches* [5], are zero-mean Gaussian random variables with

$$E\{\tilde{h}_{l_1} \cdot \tilde{h}_{l_2}^*\} = \begin{cases} \lambda_{l_1} & , \quad \text{if} \quad l_1 = l_2 \\ 0 & , \quad \text{otherwise,} \end{cases} \tag{7}$$

$\forall\, l_1, l_2 = \overline{1, L}$, so that they are independent.

The second step in MREC is maximal-ratio combining of the L components of the transformed signal vector $\tilde{\mathbf{y}}_L$. The symbol detector for MREC of order L is:

$$\hat{b}_{MREC}^{(N,L)} = \text{sign}\left[\Re\left(\left[\tilde{\mathbf{w}}_{MREC}^{(N,L)}\right]^{\mathcal{H}} \tilde{\mathbf{y}}_L\right)\right], \text{ with } \tilde{\mathbf{w}}_{MREC}^{(N,L)} = \tilde{\mathbf{h}}_L.$$

Thus, MREC is devised to employ both the eigen-structure of the long-term correlation matrix of the channel vector as well as the corresponding short-term eigenbranches. Let us indicate the relationships between MREC, Max-ASNR BF and MRC, **for perfect channel knowledge**: (1) MREC with $L = 1$ actually represents Max-ASNR BF, because then the above MREC detector coincides with the Max-ASNR BF detector from (5); (2) MREC with $L = N$ (denoted further as *full MREC*) is equivalent to MRC because then the above MREC detector coincides with the MRC detector — see also [12].

III. ANALYSIS OF EXACT MREC FOR ESTIMATED CHANNEL

Since MREC consists of maximal-ratio combining for independent eigenbranches, we apply previous results on MRC for independent channel gains to analyze MREC. It can be shown [10] that if $\tilde{h}_l$ and its estimate $\tilde{g}_l$ are jointly Gaussian the eigenbranch instantaneous SNR conditioned on $\tilde{g}_l$ is

$$\tilde{\gamma}_l \triangleq \frac{\frac{E_b}{N_0}\,\sigma_{\tilde{h}_l}^2\,|\tilde{\mu}_l|^2}{\frac{E_b}{N_0}\,\sigma_{\tilde{h}_l}^2\,(1 - |\tilde{\mu}_l|^2) + 1} \cdot \frac{|\tilde{g}_l|^2}{E\{|\tilde{g}_l|^2\}}, \tag{8}$$

where

$$\tilde{\mu}_l \triangleq \frac{\sigma_{\tilde{h}_l,\tilde{g}_l}^2}{\sqrt{\sigma_{\tilde{h}_l}^2\,\sigma_{\tilde{g}_l}^2}}. \tag{9}$$

is the correlation coefficient of the actual eigenbranch and its estimate, with $\sigma_{\tilde{h}_l,\tilde{g}_l}^2 \triangleq E\{\tilde{h}_l\,\tilde{g}_l^*\}$, $\sigma_{\tilde{h}_l}^2 \triangleq E\{|\tilde{h}_l|^2\} = \lambda_l$ and $\sigma_{\tilde{g}_l}^2 \triangleq E\{|\tilde{g}_l|^2\}$. Then [10] $\tilde{\gamma}_l$ is exponentially distributed with mean $E\{\tilde{\gamma}_l\} = \tilde{\Gamma}_l$ given by

$$\tilde{\Gamma}_l \triangleq \frac{\frac{E_b}{N_0}\lambda_l|\tilde{\mu}_l|^2}{\frac{E_b}{N_0}\lambda_l\,(1 - |\tilde{\mu}_l|^2) + 1}. \tag{10}$$

Notice that $\tilde{\mu}_l = 1$ when the lth eigenbranch is assumed perfectly-known and thus $\tilde{\Gamma}_l = \frac{E_b}{N_0}\lambda_l$.

Most previous work related to MRC for imperfect channel knowledge employed the branch estimates as actual weights for the received signals. While it simplifies implementation, this approach is actually suboptimal (approximate) for channel gains with unequal variances (unbalanced). Then, the weights for *approximate MREC* [6] [7] [9] are

$$\left[\tilde{\mathbf{w}}_{approx.\,MREC}^{(N,L)}\right]_l = \tilde{g}_l,\; l = \overline{1, L}. \tag{11}$$

Denote as $\tilde{\gamma}$ the total instantaneous output-SNR conditioned on the eigenbranch estimates for a combiner with $L \leq N$ eigenbranches. Based on results from [10] for exact MRC given the estimated channel gains, the weights for *exact MREC* given the eigen-branch estimates, i.e., for maximizing $\tilde{\gamma}$, can be shown to be

$$\left[\tilde{\mathbf{w}}_{exact\,MREC}^{(N,L)}\right]_l = \frac{\sqrt{\frac{E_b}{N_0}\,\lambda_l}\;\tilde{\mu}_l}{\frac{E_b}{N_0}\,\lambda_l\;(1 - |\tilde{\mu}_l|^2) + 1}\,\frac{\tilde{g}_l}{\sigma_{\tilde{g}_l}},\; l = \overline{1, L}, \tag{12}$$

yielding

$$\tilde{\gamma} \triangleq \sum_{l=1}^{L} \tilde{\gamma}_l. \tag{13}$$

Since in practice each eigenbranch estimate $\tilde{g}_l$ would be computed by sampling $\tilde{y}_l$, then $\tilde{\gamma}_l$, $l = \overline{1, L}$ are mutually independent, and the AEP for exact MREC with N branches and L eigenbranches can be shown to be

$$P_e^{(N,L)} = \frac{1}{\pi}\int_0^{\pi/2} \prod_{l=1}^{L} \frac{\sin^2\phi}{\sin^2\phi + \tilde{\Gamma}_l}\,\mathrm{d}\phi, \tag{14}$$

by employing the p.d.f. of $\tilde{\gamma}$ to average the instantaneous error probability over the fading as in [3, Section 9.2.3.1] [7]. This AEP expression was used in [7] to devise a natural criterion for adaptive order selection in MREC, which trades-off detection performance and processing complexity.

For perfect channel knowledge we know that MREC with $L = 1$ is equivalent to Max-SNR BF, and that full MREC ($L = N$) is equivalent to MRC. Then, using (14) and the Facts from Section II it can be shown that balanced uncorrelated branches minimize the AEP for MRC, while coherent branches maximize it. The opposite can be shown for Max-ASNR BF.

The AEP-expression from (14) can be specialized for PSAM-based estimation [11], in which the receiver interpolates the signal samples acquired during the intervals corresponding to the pilot symbols. The notation (k, m) is used for temporal indexing: $k = \overline{-K_1, K_2}$ is the slot index; k = 0 for the slot in which estimation takes place; $K = K_1 + K_2 + 1$ frames are used for interpolation; M = slot length; m =

$\overline{0, M-1}$ is the symbol index in a slot, $m = 0$ for the pilot symbol. For MREC, the lth eigenbranch at the mth data-symbol position in the slot can be estimated as

$$\tilde{g}_l(0, m) = \tilde{\mathbf{v}}_l^{\mathcal{H}}(m)\, \tilde{\mathbf{r}}_l, \tag{15}$$

where $\tilde{\mathbf{v}}_l(m)$ is the PSAM interpolation filter, $\tilde{\mathbf{r}}_l \triangleq \frac{1}{\sqrt{E_b \cdot b_p}} [\tilde{y}_l(-K_1, 0) \ldots \tilde{y}_l(K_2, 0)]^{\mathcal{T}}$, b_p is the pilot symbol and $\tilde{y}_l(k, 0) = \mathbf{e}_l^{\mathcal{H}} \mathbf{y}(k, 0)$.

We consider two types of interpolation filters: (1) the Wiener filter, which is MMSE optimum in the presence of noise and depends on the second-order statistics of the received signals [11] and (2) the filter with SINC-type impulse response, which is optimum in the absence of noise and independent of the received signals, tapered by a raised-cosine [13]. Denote the corresponding estimation methods as MMSE PSAM and SINC PSAM. The coefficients of the above interpolation filters and the correlations required to compute $\tilde{\mu}_l$, $l = \overline{1, L}$ from (9), which enter the AEP-formula (14) through $\tilde{\Gamma}_l$ from (10), were determined and are shown in Tables I – III from [6] [7]. Note that the estimate from (15), and thus the AEP, depends on the position of the detected symbol in the slot, m.

Remarks: It can be shown that $\lambda_l \approx 0$ leads to $\tilde{g}_l \approx 0$ for MMSE PSAM, but not for SINC PSAM, and that the factor multiplying $\tilde{g}_l$ in (12) is nearly-zero for SINC PSAM, but not for MMSE PSAM. Therefore, for **exact MREC** the detection performance does not degrade when adding a new eigenbranch, a fact also indicated by (14). On the other hand, eigenbranches corresponding to very small eigenvalues in **approximate MREC** may degrade the detection performance for SINC PSAM, but not for MMSE PSAM [6] [7].

IV. Numerical results

For the example setting described in Section II and exact combining for normalized maximum Doppler frequency $f_n = 0.05$, symbol SNR $E_b/N_0 = 5\,\text{dB}$ and MMSE PSAM with $M = 7$ and $K = 11$ [7] [11], Fig. 2 shows: with dashed lines — the AEP for MREC, i.e., $P_e^{(N,L)}(\Delta)$ from (14) for $L = \overline{1, N}$; with thick solid line — the AEP for MRC, from an expression obtained as indicated in [7]; with dotted solid line — the AEP for MREC with order L selected using the performance/complexity trading-off method proposed in [7]. These curves were obtained by averaging the AEPs over a slot, i.e., for $m = \overline{1, M-1}$. In [7] we plotted the AEP from (14) for both MMSE and SINC PSAM for Laplacian AOA distribution.

To understand Fig. 2, recall from Section II that as the AOA dispersion increases the correlation between the branches decreases and the intended-signal energy is distributed into a larger-dimensional subspace (see Fig. 1). Given $L > 1$, MREC yields diversity gain and therefore its AEP-performance improves when Δ increases from 0, until the actual dimension of the signal subspace increases beyond L, leading to AEP degradation. Given Δ, L-order MREC performs as well as full MREC only if L is large enough. As expected, exact full MREC offers minimum AEP throughout the AOA-dispersion

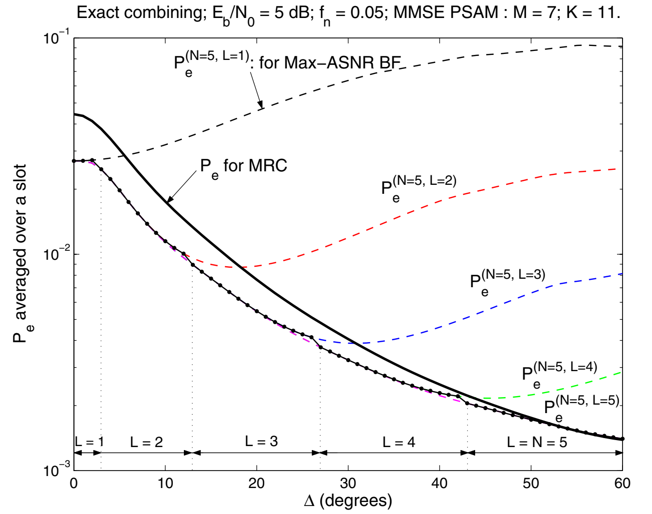

Fig. 2. Dashed lines — AEP for exact MREC, $P_e^{(N,L)}$, $N = 5, L = \overline{1, N}$, calculated with (14), vs. the maximum AOA dispersion, when MMSE PSAM is used for estimation. Thick solid line — the AEP for exact MRC obtained as in [7]. Dotted solid line — AEP obtained when the order L for exact MREC is selected with the criterion proposed in [7].

range. On the other hand, since (14) with $L = 1$ expresses the AEP for Max-ASNR BF, Fig. 2 indicates that MREC with $L \geq 2$ may significantly outperform Max-ASNR BF for AOA dispersion larger than a few degrees.

Notice also that for exact combining, for each $L \leq N$, MREC has lower BER than MRC up to some value of Δ, and full MREC appears at least as effective as MRC regardless of Δ, i.e., of branch correlation. The explanation is that, for significantly-correlated channel gains, a few eigenbranches have higher average SNR and therefore are estimated more accurately compared to the branches [5]. Furthermore, compared to MRC, MREC may significantly reduce processing since updating the eigen-structure estimate does not increase complexity significantly as it occurs infrequently relative to the rate at which the eigenbranch estimates are updated [5].

Using (14) and results from [6] [7] we can also plot the AEPs vs. the symbol SNR, E_b/N_0. (Such plots are not provided here because of space limitations, but they resemble the corresponding ones shown in [7] for Laplacian AOA distribution.) For the same example setting, at $AEP = 10^{-2}$ and $\Delta = 10°$, we found exact MREC of order $L = 2$ to be about 5 dB better than Max-ASNR BF and about 1 dB better than exact MRC, for both MMSE and SINC PSAM. We noticed that the performance gap between MREC of a given order $L > 1$ and Max-ASNR BF/MRC increases/decreases with E_b/N_0, which can be explained easily using diversity order/gain considerations, as in [7].

Next, we present Monte Carlo simulation results for exact MREC, Max-ASNR BF and MRC. Fig. 3 shows the bit-error-rate (BER) for exact MREC and MRC when PSAM with the MMSE and SINC interpolation filters are used for estimation. For the same antenna geometry and system parameters as for

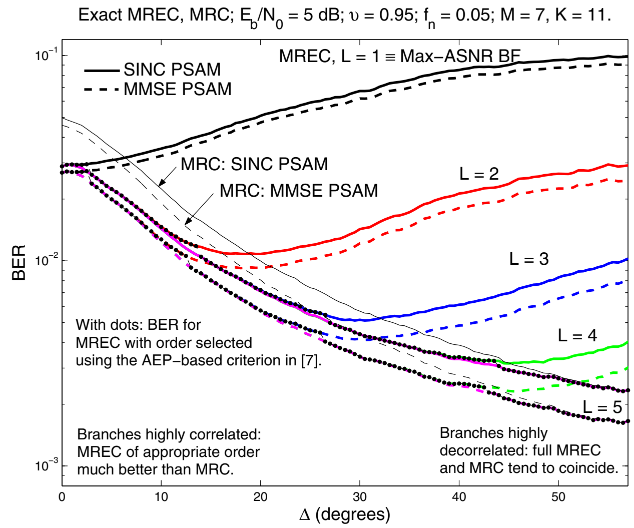

Fig. 3. BER vs. the maximum AOA dispersion, obtained by simulation for exact MREC and MRC, for MMSE and SINC PSAM estimation.

Figs. 1 and 2 we generated the channel model in (2) for about 10^5 bits at each value of Δ. The BER-curves for MREC with MMSE PSAM agree with the AEP-curves obtained with (14) and shown in Fig. 2, confirming our analysis. Fig. 3 also shows, with dots, the BER obtained for exact MREC with order selected using the method in [7]: clearly, the signal processing requirements in MREC can be efficiently adapted to the actual environment by choosing the lowest number of eigenbranches that meets a target BER — see [7] for more details.

Note that for uncorrelated branches full MREC reduces to MRC, which is reflected in Figs. 2 and 3 by the similar AEP/BER-performance of MRC and full MREC for large AOA dispersion. On the other hand, Fig. 3 confirms that even order-2 MREC can considerably improve the BER at a low extra complexity compared to Max-ASNR, even if the branches are highly correlated (see also Fig. 1).

For **approximate** MREC with MMSE PSAM, other AEP/BER plots (not shown here) indicate that, given the AOA dispersion, overestimating the order L increases the complexity but never degrades the detection performance [6] [7]. Thus, approximate MREC with MMSE PSAM functions as exact MREC. On the other hand, overestimating the order for approximate MREC with SINC PSAM estimation not only increases complexity, but degrades the detection performance as well [6] [7]. These observations are explained by the remarks at the end of the previous section. An in-depth analysis of approximate MREC appears in [6] [7].

V. Conclusions

The paper analyzes maximal-ratio eigen-combining (MREC), which was recently proposed as an alternative to conventional maximum average-SNR beamforming (Max-ASNR BF) as well as maximal-ratio combining (MRC) in scenarios with partially-correlated channel gains. We provide a general AEP-expression for exact MREC in the case of BPSK signals and imperfectly-estimated, partially-correlated Rayleigh-fading channel gains, and we specialize it for pilot-symbol-aided channel estimation. For antenna array systems, numerical results obtained from the analysis and by simulation indicate that even low-complexity MREC can outperform Max-ASNR BF considerably if the angle-of-arrival (AOA) dispersion is more than a few degrees. Furthermore, exact MREC is always at least as effective as exact MRC, with more substantial performance and complexity benefits at low symbol-SNR for channel gains with significant correlation (greater than 0.8).

Acknowledgement

This research has been sponsored by the Natural Sciences and Engineering Research Council of Canada, grant 41731-00, Bell University Labs and by Samsung AIT.

References

[1] J. Salz and J. H. Winters, "Effect of fading correlation on adaptive arrays in digital mobile radio," *IEEE Trans. Veh. Technol.*, vol. 43, no. 4, pp. 1049 –1057, Nov. 1994.

[2] R. A. Monzingo and T. W. Miller, *Introduction to Adaptive Arrays*. New York, NY: John Wiley, 1980.

[3] M. Simon and M.-S. Alouini, *Digital Communications over Fading Channels. A Unified Approach to Performance Analysis*. New York, NY: John Wiley and Sons, Inc., 2000.

[4] M. Kim, W.-C. Lee, J. Choi, and S. Choi, "Adaptive beamforming technique based on eigen-space method for a smart antenna in IS2000 1X environment," in *Antennas and Propagation Society International Symposium*, vol. 1, 2002, pp. 118–121.

[5] J. S. Hammerschmidt, C. Brunner, and C. Drewes, "Eigenbeamforming — a novel concept in array signal processing," in *Proc. European Wireless Conference 2000*, Dresden, Germany, Sept. 2000.

[6] C. Siriteanu and S. D. Blostein, "Maximal-ratio eigen-combining: a performance analysis," *Canadian Journal of Electrical and Computer Engineering*, vol. 29, no. 1/2, Jan./Apr. 2004. [Online]. Available: http://ipcl.ee.queensu.ca

[7] ——, "Performance of smart antenna arrays with maximal-ratio eigen-combining," Queen's University, Department of Electrical and Computer Engineering, Kingston, Ontario, Canada, Tech. Rep. 0401, Jan. 2004. [Online]. Available: http://ipcl.ee.queensu.ca

[8] R. A. Haddad and T. W. Parsons, *Digital signal processing: theory, applications, and hardware*. New York, NY: Computer Science Press, an imprint of W. H. Freeman and Co., 1991.

[9] F. A. Dietrich and W. Utschick, "Maximum ratio combining of correlated Rayleigh fading channels with imperfect channel knowledge," *IEEE Commun. Lett.*, vol. 7, no. 9, pp. 419–421, Sept. 2003.

[10] P. Polydorou and P. Ho, "Error performance of MPSK with diversity combining in non-uniform Rayleigh fading and non-ideal channel estimation," in *Vehicular Technology Conference Proceedings, VTC 2000-Spring*, vol. 1, Tokyo, May 2001, pp. 627–631.

[11] J. K. Cavers, "An analysis of pilot symbol assisted modulation for Rayleigh fading channels," *IEEE Trans. Veh. Technol.*, vol. 40, no. 4, pp. 686–693, Nov. 1991.

[12] X. Dong and N. Beaulieu, "Optimal maximal ratio combining with correlated diversity branches," *IEEE Commun. Lett.*, vol. 6, no. 1, pp. 22–24, Jan. 2002.

[13] N. W. K. Lo, D. D. Falconer, and A. U. H. Sheikh, "Adaptive equalization and diversity combining for mobile radio using interpolated channel estimates," *IEEE Trans. Veh. Technol.*, vol. 40, no. 3, pp. 636–645, Aug. 1991.